MRS Communications (2015), *5*, 435–440
© Materials Research Society, 2015
doi:10.1557/mrc.2015.49

MRS Communications

Polymers/Soft Matter Research Letter

Effects of alkyl chain positioning on conjugated polymer microstructure and field-effect mobilities

Bob C. Schroeder† and **Christian B. Nielsen,** Department of Chemistry and Centre for Plastic Electronics, Imperial College London, London SW7 2AZ, UK
Paul Westacott, Department of Materials and Centre for Plastic Electronics, Imperial College London, London SW7 2AZ, UK
Jeremy Smith, Stephan Rossbauer, and **Thomas D. Anthopoulos,** Department of Physics and Centre for Plastic Electronics, Imperial College London, London SW7 2AZ, UK
Natalie Stingelin, Department of Materials and Centre for Plastic Electronics, Imperial College London, London SW7 2AZ, UK
Iain McCulloch, Department of Chemistry and Centre for Plastic Electronics, Imperial College London, London SW7 2AZ, UK; Physical Sciences and Engineering Division, King Abdullah University of Science and Technology (KAUST), Thuwal, Saudi Arabia

Address all correspondence to Bob C. Schroeder at **bschroeder@stanford.edu**

(Received 3 June 2015; accepted 19 June 2015)

Abstract

Solubilizing alkyl chains play a crucial role in the design of semiconducting polymers because they define the materials solubility and processability as well as both the crystallinity and solid-state microstructure. In this paper, we present a scarcely explored design approach by attaching the alkyl side chains on one side (cis-) or on both sides (trans-) of the conjugated backbone. We further investigate the effects of this structural modification on the solid-state properties of the polymers and on the charge-carrier mobilities in organic thin-film transistors.

Introduction

The incorporation of fused conjugated monomers into semiconducting polymers has attracted significant attention in recent years, especially for organic field-effect transistor (FET) applications[1–4]. By fixing multiple aromatic units via covalent bridging bonds, it is possible to eliminate torsional angles between adjacent units, which correspondingly leads to significantly reduced energetic disorder[5]. Sirringhaus and co-workers recently provided evidence that such collinear conjugated building blocks are essential to limit conformational disorder along conjugated polymer chains, which turned out to be a prerequisite to achieve high charge-carrier mobilities in organic FETs[6].

The fusion of multiple aromatic units into rigid ladder-type building blocks however typically leads to a significant reduction in material solubility. Synthetically the reduction in solubility can be minimized or even prevented by flanking the fused ring system with solubilizing alkyl side chains[7,8]. Unfortunately there is no universal approach applicable to every collinear monomer, but rather the side chain has to be judiciously chosen depending on the desired property. Even though the side chains have only a minimal effect on the overall electronic properties of a conjugated polymer, they play a key role in defining the solid-state properties and material processability. Alkyl chains are the most commonly used solubilizing groups, mainly for their electronic neutrality and their ease of synthesis. Whereas branched alkyl solubilizing groups are commonly used for organic photovoltaic applications, long linear side chains are often preferred for FET applications, as the less sterically hindering nature of a linear alkyl side chain leads to denser solid-state packing, more intermolecular short contacts, and thus potentially to higher charge-carrier mobilities[9].

Another important decision to make when designing the solubilizing groups of semiconducting polymers, is the hybridization of the anchoring atom. If the side chains are attached via a sp^2-hybridized carbon to the polymer backbone, then the alkyl chains will be in the same plane as the conjugated backbone, which favors the formation of highly crystalline, long-ranged ordered domains[10–13]. Even though this design could lead to reduced solubility because only one side chain per anchoring carbon can be attached, it can be highly desirable for charge transport because the formation of three dimensionally ordered film is now feasible[14,15]. The alternative to sp^2-hybridized anchoring atoms would be a sp^3-hybridized atom. Because of the tetrahedral nature of the sp^3-hybridization, the alkyl chains would no longer be in the same plane as the conjugated backbone. This architecture prevents to some extent the intermolecular chain packing, thus significantly increasing the polymer solubility. Furthermore the sp^3-hybridization allows two solubilizing chains per anchoring atom on the backbone which further enhances the materials solubility[16].

† Current address: Department of Chemical Engineering, Stanford University, 443 Via Ortega, Stanford, California 94305.

https://doi.org/10.1557/mrc.2015.49 Published online by Cambridge University Press

Multiple studies have been performed on the effect of different alkyl chains and anchoring architectures on molecular packing and charge-carrier mobilities[17–21]. However, there has been little research on how the side-chain arrangement along the conjugated backbone alters the electronic performance. In this paper, we were interested in elucidating this property by synthesizing two structurally similar polymers, one containing thieno[3,2-*b*]thienobis(silolothiophene) (Si4T) building blocks in the polymer backbone and the other containing dithienosilolothiophene (Si3T)[22,23]. Even though both building blocks are structurally very similar, their main difference is the side-chain arrangement along the fused monomer. Whereas in the case of Si4T, the side chains are attached on either side of the conjugated structure (trans-), the particular geometry of the Si3T building block allowed for a cis-arrangement as illustrated in Fig. 1.

In this study, we will therefore focus on the effects of cis- and trans-side-chain arrangement along two structurally similar polymer backbones and how this structural difference influences the materials microstructure and ultimately the charge-carrier mobilities in thin-film organic FETs.

Experimental details

All chemicals were purchased from Sigma-Aldrich, Alfa Aesar, or Fluorochem and used without further purification. The Si3T and Si4T monomers were synthesized according to previously published methods[22,23]. The Stille coupling polymerizations were performed according to previously described procedures[24]. Number-average (M_n) and weight-average (M_w) molecular weights were determined with an Agilent Technologies 1200 series SEC in chlorobenzene at 80 °C, using two PL mixed B columns in series. The SEC was calibrated against narrow weight-average dispersity ($Đ < 1.10$) polystyrene standards. The UV–vis absorption spectra were recorded on a UV-1601 Shimadzu spectrometer. Differential scanning calorimetry (DSC) experiments were carried out with a TA Instruments DSC Q20 using Tzero Aluminum pans and a heating rate of 10 °C/min. Photoelectron spectroscopy in air (PESA) measurements were recorded with a Riken Keiki AC-2 PESA spectrometer with a power setting of 5 nW and a power number of 0.5. X-ray diffraction (XRD) measurements were carried out with a PANALYTICAL X'PERT-PRO MRD diffractometer equipped with a nickel-filtered Cu $K_{\alpha 1}$ beam and an X' CELERATOR detector, using a current of 40 mA and an accelerating voltage of 40 kV. Top-gate, bottom-contact organic FETs were fabricated on the glass with 2,3,4,5,6-pentafluorothiophenol-treated gold electrodes, CYTOP (900 nm) dielectric, and Al gate. Polymer films were spin cast from *o*-dichlorobenzene (10 mg/mL) solutions at a speed of 2000 rpm and annealed at 200 °C for 15 min. The carrier mobility of the films was evaluated by measuring transfer curves in saturation ($V_{DS} = -60$ V) using a Keithley 4200 semiconductor parameter analyzer. The saturation mobility was determined by fitting a linear relationship of the square root of the drain current to gate potential in the range of −40 to −60 V.

Results and discussion

The synthetic routes toward monomers Si3T and Si4T were published elsewhere[22,23]. The stannylated monomers were polymerized under Stille cross-coupling conditions with the corresponding dibrominated monomer, 4,7-bis(5-bromothiophen-2-yl)benzo[*c*][1,2,5] thiadiazole (DTBT). The synthetic scheme toward both polymers, Si3T–DTBT and Si4T–DTBT, is presented in Scheme 1. Both polymers were obtained with reasonable molecular weights (Table I) as dark blue fibrous solids.

The UV–vis absorption spectra of both polymers were recorded in diluted chlorobenzene solution and in thin films on the glass (Fig. 2). The detailed absorption data and related band gaps are presented in Table II. Both polymers show similar absorption bands in the solution and in the solid state, with a major intramolecular charge-transfer band between 600 and 800 nm.

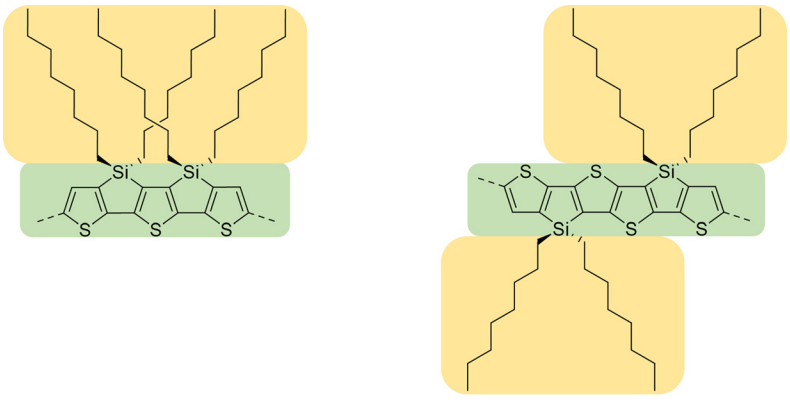
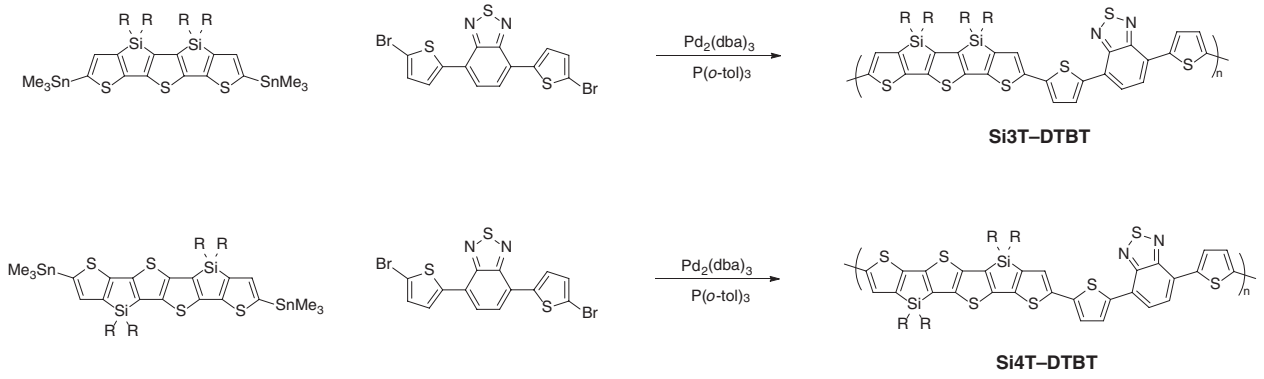


Figure 1. Chemical structures of both polycyclic fused donor moieties. The planar conjugated backbones are highlighted in green and the out of plane solubilizing alkyl chains are highlighted in yellow.

https://doi.org/10.1557/mrc.2015.49 Published online by Cambridge University Press



Scheme 1. Synthetic route toward Si3T–DTBT and Si4T–DTBT polymers.

Table I. Molecular weights of Si3T–DTBT and Si4T–DTBT polymers.

Polymer	M_n (kg/mol)[a]	M_w (kg/mol)[b]	$Đ_w$[c]
Si3T–DTBT	12	34	2.8
Si4T–DTBT	21	38	1.8

[a]Number-average molecular weight.
[b]Weight-average molecular weight.
[c]Weight dispersity defined as M_w/M_n.

The π–π* transitions in both cases are broadened and appear as a shoulder of the main absorption peak about 500 nm. The most interesting difference arises from the solution spectra of both polymers. The Si3T–DTBT polymer is red-shifted by 32 nm compared with the Si4T–DTBT polymer. This bathochromic shift could be explained by polymer aggregation in solution, which would lead to extended conjugation due to a backbone planarization. Contrary to the Si4T–DTBT polymer, the conjugated backbone of Si3T–DTBT is more accessible for π–π interactions in solution because of the cis-attachment of the alkyl side chains. In the solid state, however, this effect seems to be less important and both polymers present nearly identical absorption spectra. This could in part be because the solidification process is driven by intermolecular π–π interactions which will reduce conformational disorder, independent of the alkyl side chains attachment. The optical band gaps for both polymers were extracted from the absorption onsets of the solid-state absorption spectra and estimated to be 1.6 eV in both cases.

The frontier energy levels were measured by PESA measurements. Because of the more aromatic nature of the central thieno[3,2-*b*]thiophene unit in Si4DT compared with the central thiophene ring in the Si3T monomer, the formation of the quinoidal structure should be less favored in the Si4T–DTBT polymer leading to a slight stabilization of the highest occupied molecular orbital (HOMO). This assumption however could not be experimentally verified by PESA and the ionization potential for both polymers were measured to be 5.0 eV.

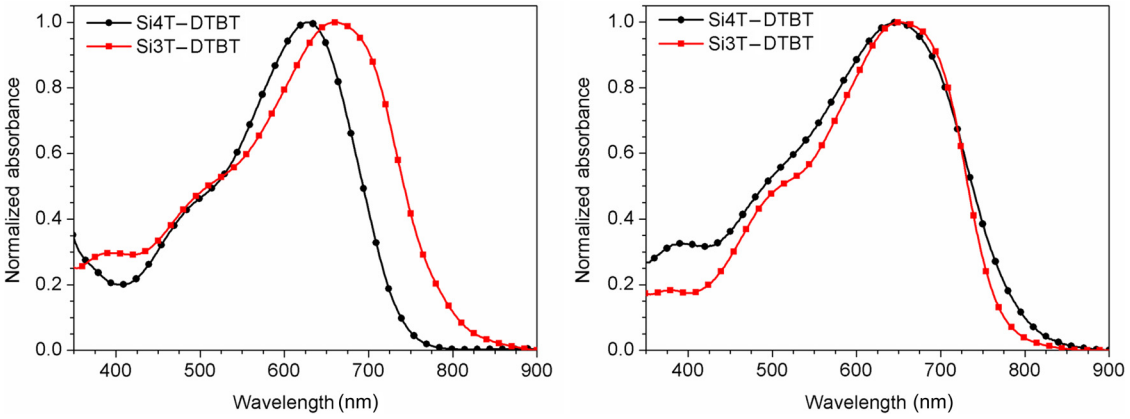


Figure 2. UV–vis absorption spectra of polymers Si3T–DTBT and Si4T–DTBT in diluted chlorobenzene solution (left) and in thin films on the glass substrate (right).

https://doi.org/10.1557/mrc.2015.49 Published online by Cambridge University Press

Table II. Optical properties of Si3T–DTBT and Si4T–DTBT polymers.

Polymer	λ_{max} soln (nm)[a]	λ_{max} film (nm)[b]	IP/EA (eV)[c]	E_g^{opt} (eV)
Si3T–DTBT	660	651	−5.0/−3.4	1.6
Si4T–DTBT	628	649	−5.0/−3.4	1.6

[a]Measured in dilute chlorobenzene solution.

[b]Spin-coated from 5 mg/mL chlorobenzene solution on the glass substrate.

[c]The electron affinity (EA) is estimated by adding the absorption onset to the ionization potential (IP).

Density-functional theory calculations were performed at the B3LYP/6-31G* level to gather a better understanding about the HOMO and lowest unoccupied molecular orbital (LUMO) wave function distributions as well as the geometry of the polymer backbones. The energy-minimized structures are shown in Fig. 3, as well as the HOMO and LUMO wave function distributions. Both polymers have a low-amplitude zigzag-shaped backbone with no substantial torsional angles between the different aromatic building blocks. The molecular modeling further confirmed our design strategy because the Si4T–DTBT backbone is decorated on both sides with alkyl chains, contrary to the Si3T–DTBT where all the alkyl chains are arranged along one side of the backbone, thus making the backbone more accessible for intermolecular interactions. It is noteworthy that these calculations were performed on energy-minimized trimers and might present an overly idealized representation of the molecular packing. In an actual polymer film, the polymer chains are likely to not exclusively pack in this energy-minimized structure, but rotations along the polymer backbone could lead to an inhomogeneous distribution of the alkyl side chains along the conjugated backbone. The HOMO wave functions are distributed along the electron-rich conjugated backbone in both polymers, whereas the LUMO orbitals are preferentially located on the electron-deficient benzothiadiazole units.

After the optical measurements and theoretical calculations were in good agreement with our anticipated design strategy, we investigated the physical properties and solid-state microstructure further. DSC measurements did not reveal any phase transitions in the measured temperature range (0–300 °C). Furthermore, we probed drop-casted polymer films by XRD and the corresponding diffractograms are represented in Fig. 4.

The Si3T–DTBT polymer showed sharp diffraction peaks at low angles, whereas the diffraction peaks for the Si4T–DTBT polymer were extremely weak and broad. Even after thermal annealing the diffraction pattern of Si4T–DTBT remained nearly featureless, whereas the diffraction peaks for Si3T–DTBT sharpened and intensified. The lamellar stacking distance of Si4T–DTBT is slightly smaller (15.0 Å) than for Si3T–DTBT (18.5 Å). One possible explanation for this observation could be partial side-chain interdigitation, which could lead to a shortening of the lamellar stacking distances. The cis-side-chain arrangement is denser along the polymer backbone and could prevent side-chain interdigitation, thus leading to a longer distance of periodicity along the (1 0 0)-axis. Thermal annealing increased the lamellar stacking distances slightly for both polymers (19.9 Å for Si3T–DTBT and 16.2 Å for Si4T–DTBT), but did not seem to have any positive effect on the π-stacking diffraction peaks which remained unidentifiable.

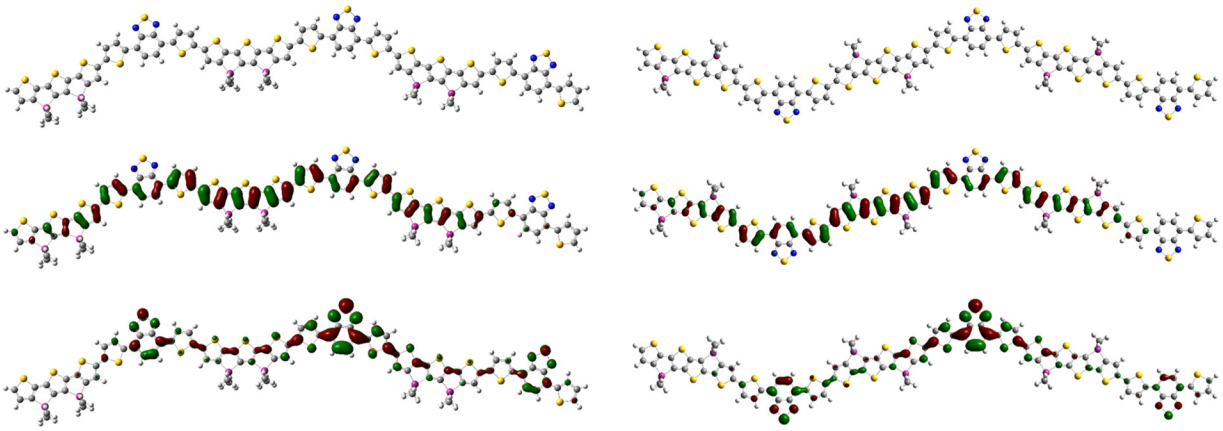


Figure 3. Energy-minimized structures (B3LYP/6-31G*) of methyl-substituted Si3T–DTBT (left column) and Si4T–DTBT (right column) trimers with HOMO (middle row) and LUMO (bottom row) wave function visualizations, respectively.

https://doi.org/10.1557/mrc.2015.49 Published online by Cambridge University Press

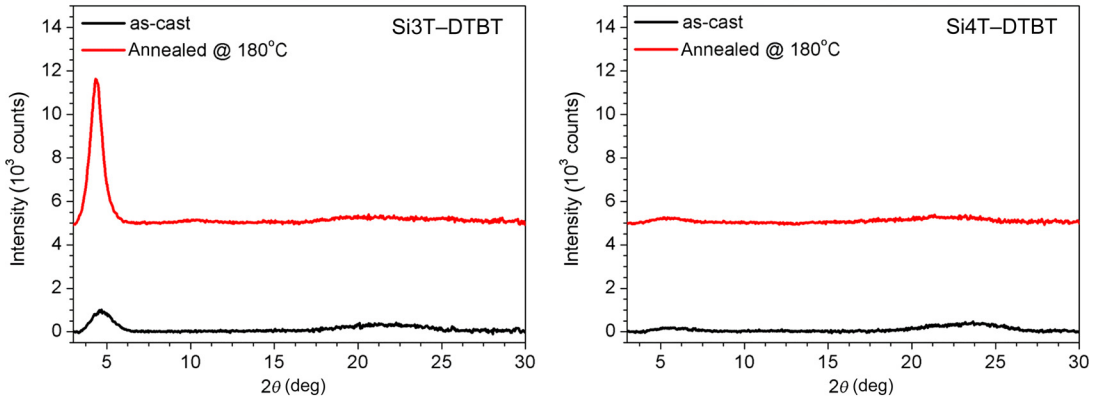


Figure 4. XRD patterns of drop-casted films (10 mg/mL in chlorobenzene) on the silicon substrate of Si3T–DTBT (left) and Si4T–DTBT (right). As-cast films are shown in black and annealed films (10 min at 180 °C) are shown in red (the red curves are shifted for clarity).

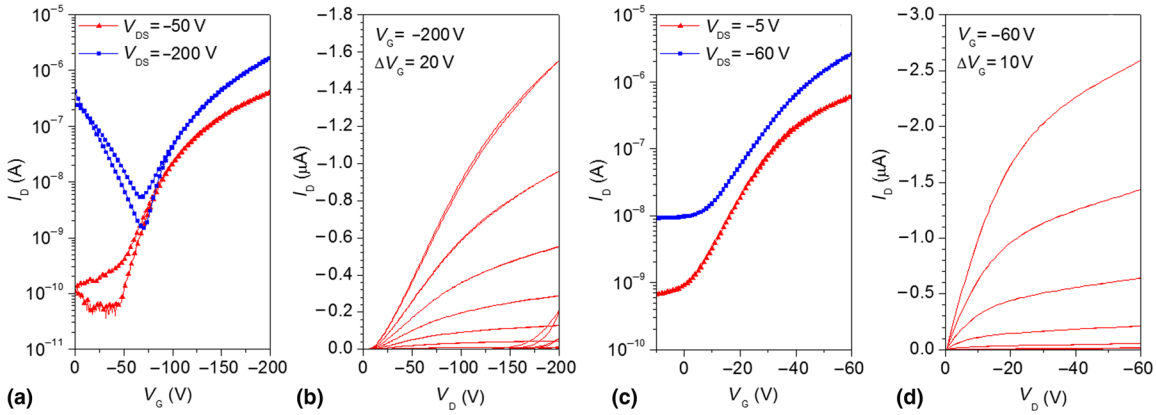


Figure 5. Transfer curves and output characteristics of Si3T–DTBT (A, B) and Si4T–DTBT (C, D) in top-gate, bottom-contact organic field effect transistor devices.

Table III. Organic FET properties of Si3T–DTBT and Si4T–DTBT polymers.

Polymer	μ_{sat} (cm^2/Vs)[a]	μ_{lin} (cm^2/Vs)[b]	I_{on}/I_{off}[c]	V_T (V)
Si3T–DTBT	$1.4\ (\pm0.5) \times 10^{-3}$	$0.8\ (\pm0.2) \times 10^{-3}$	$\sim10^4$	−95
Si4T–DTBT	$8.8\ (\pm0.4) \times 10^{-2}$	$7.4\ (\pm0.6) \times 10^{-2}$	$\sim10^3$	−21

[a]μ_{sat} refer to the highest effective hole mobilities measured in the saturation regime.
[b]μ_{lin} refer to the highest effective hole mobilities measured in the linear regime.
[c]The on-to-off ratios (I_{on}/I_{off}) were extracted from the linear regime.

We fabricated top-gate, bottom-contact organic FETs with 2,3,4,5,6-pentafluorothiophenol-treated gold electrodes and CYTOP dielectric. The polymers were spin-coated from *o*-dichlorobenzene and annealed at 200 °C prior to the measurement. The Si4T–DTBT polymer formed smooth homogeneous films, whereas the Si3T–DTBT films suffered from dewetting. As a result of the poor film quality, the Si3T–DTBT devices showed substantial gate leakage and higher voltages were needed to drive the device, making the mobility determination rather difficult (Fig. 5 and Table III). Even though the Si4T–DTBT polymer was less crystalline than the Si3T–DTBT polymer, the extracted hole mobilities were one order of magnitude higher. However, this is likely the result of the better film quality obtained for the Si4T–DTBT polymer. Why exactly the Si3T–DTBT polymer is suffering from substrate dewetting remains a matter of speculation, one possible

https://doi.org/10.1557/mrc.2015.49 Published online by Cambridge University Press

explanation however could be the lower molecular weight of Si3T–DTBT which lead to lower viscosity solutions compared with Si4T–DTBT solutions.

Conclusion

We successfully synthesized and studied the cis-, respectively, trans-side-chain arrangements along two different conjugated polymer backbones. Our results proved that this could be a viable design approach to enhance interchain polymer aggregation and could lead to significant crystallinity enhancements. We furthermore expect this approach to be of high significance for the design of new conjugated polymers because not only does our approach allow us to significantly minimize the torsional disorder along the polymer backbone, but also at the same time it is an elegant approach to tune the materials microstructure. This will not only be of interest for organic FET applications, but could also play a crucial role in gaining more control over the microstructure in organic photovoltaic devices.

Acknowledgments

The authors would like to thank Dr. Scott Watkins at CSIRO for performing the PESA measurements. B. C. S. acknowledges the National Research Fund of Luxembourg and the EPSRC Knowledge Transfer Secondment Scheme for financial support. This work was in part carried out under the EPSRC Projects EP/F056710/1, EP/I019278/1, and EP/G037515/1 with support from the Centre for Plastic Electronics at Imperial.

References

1. H. Sirringhaus: Organic field-effect transistors: the path beyond amorphous silicon. *Adv. Mater.* **26**, 1319 (2014).
2. W. Wu, Y. Liu, and D. Zhu: π-conjugated molecules with fused rings for organic field-effect transistors: design, synthesis and applications. *Chem. Soc. Rev.* **39**, 1489 (2010).
3. C.B. Nielsen and I. McCulloch: Recent advances in transistor performance of polythiophenes. *Progr. Polym. Sci.* **38**, 2053 (2013).
4. S. Holliday, J.E. Donaghey, and I. McCulloch: Advances in charge carrier mobilities of semiconducting polymers used in organic transistors. *Chem. Mater.* **26**, 647 (2014).
5. X. Zhang, H. Bronstein, A.J. Kronemeijer, J. Smith, Y. Kim, R.J. Kline, L. J. Richter, T.D. Anthopoulos, H. Sirringhaus, K. Song, M. Heeney, W. Zhang, I. McCulloch, and D.M. DeLongchamp: Molecular origin of high field-effect mobility in an indacenodithiophene-benzothiadiazole copolymer. *Nat. Commun.* **4**, 3238 (2013).
6. D. Venkateshvaran, M. Nikolka, A. Sadhanala, V. Lemaur, M. Zelazny, M. Kepa, M. Hurhangee, A.J. Kronemeijer, V. Pecunia, I. Nasrallah, I. Romanov, K. Broch, I. McCulloch, D. Emin, Y. Olivier, J. Cornil, D. Beljonne, and H. Sirringhaus: Approaching disorder-free transport in high-mobility conjugated polymers. *Nature* **515**, 384 (2014).
7. J. Mei and Z. Bao: Side chain engineering in solution-processable conjugated polymers. *Chem. Mater.* **26**, 604 (2014).
8. T. Lei, J.-Y. Wang, and J. Pei: Roles of flexible chains in organic semiconducting materials. *Chem. Mater.* **26**, 594 (2014).
9. H. Bronstein, D.S. Leem, R. Hamilton, P. Woebkenberg, S. King, W. Zhang, R.S. Ashraf, M. Heeney, T.D. Anthopoulos, J. de Mello, and I. McCulloch: Indacenodithiophene-co-benzothiadiazole copolymers for high performance solar cells or transistors via alkyl chain optimization. *Macromolecules* **44**, 6649 (2011).
10. B.S. Ong, Y. Wu, P. Liu, and S. Gardner: High-performance semiconducting polythiophenes for organic thin-film transistors. *J. Am. Chem. Soc.* **126**, 3378 (2004).
11. I. McCulloch, M. Heeney, C. Bailey, K. Genevicius, I. MacDonald, M. Shkunov, D. Sparrowe, S. Tierney, R. Wagner, W. Zhang, M. L. Chabinyc, R.J. Kline, M.D. McGehee, and M.F. Toney: Liquid-crystalline semiconducting polymers with high charge-carrier mobility. *Nat. Mater.* **5**, 328 (2006).
12. L. Biniek, B.C. Schroeder, J.E. Donaghey, N. Yaacobi-Gross, R.S. Ashraf, Y.W. Soon, C.B. Nielsen, J.R. Durrant, T.D. Anthopoulos, and I. McCulloch: New fused bis-thienobenzothienothiophene copolymers and their use in organic solar cells and transistors. *Macromolecules* **46**, 727 (2013).
13. Z. Fei, P. Pattanasattayavong, Y. Han, B.C. Schroeder, F. Yan, R.J. Kline, T. D. Anthopoulos, and M. Heeney: Influence of side-chain regiochemistry on the transistor performance of high-mobility, all-donor polymers. *J. Am. Chem. Soc.* **136**, 15154 (2014).
14. R.J. Kline, D.M. DeLongchamp, D.A. Fischer, E.K. Lin, L.J. Richter, M. L. Chabinyc, M.F. Toney, M. Heeney, and I. McCulloch: Critical role of side-chain attachment density on the order and device performance of polythiophenes. *Macromolecules* **40**, 7960 (2007).
15. L. Zhang, N.S. Colella, F. Liu, S. Trahan, J.K. Baral, H.H. Winter, S.C. B. Mannsfeld, and A.L. Briseno: Synthesis, electronic structure, molecular packing/morphology evolution, and carrier mobilities of pure oligo-/poly (alkylthiophenes). *J. Am. Chem. Soc.* **135**, 844 (2013).
16. I. McCulloch, R.S. Ashraf, L. Biniek, H. Bronstein, C. Combe, J. E. Donaghey, D.I. James, C.B. Nielsen, B.C. Schroeder, and W. Zhang: Design of semiconducting indacenodithiophene polymers for high performance transistors and solar cells. *Acc. Chem. Res.* **45**, 714 (2012).
17. H.N. Tsao, D.M. Cho, I. Park, M.R. Hansen, A. Mavrinskiy, D.Y. Yoon, R. Graf, W. Pisula, H.W. Spiess, and K. Müllen: Ultrahigh mobility in polymer field-effect transistors by design. *J. Am. Chem. Soc.* **133**, 2605 (2011).
18. T. Lei, J.-H. Dou and J. Pei: Influence of alkyl chain branching positions on the hole mobilities of polymer thin-film transistors. *Adv. Mater.* **24**, 6457 (2012).
19. J. Mei, D.H. Kim, A. Ayzner, M.F. Toney, and Z. Bao: Siloxane-terminated solubilizing side chains: bringing conjugated polymer backbones closer and boosting hole mobilities in thin-film transistors. *J. Am. Chem. Soc.* **133**, 20130 (2011).
20. I. Meager, R.S. Ashraf, S. Mollinger, B.C. Schroeder, H. Bronstein, D. Beatrup, M.S. Vezie, T. Kirchartz, A. Salleo, J. Nelson, and I. McCulloch: Photocurrent enhancement from diketopyrrolopyrrole polymer solar cells through alkyl-chain branching point manipulation. *J. Am. Chem. Soc.* **135**, 11537 (2013).
21. S. Himmelberger, D.T. Duong, J.E. Northrup, J. Rivnay, F.P.V. Koch, B. S. Beckingham, N. Stingelin, R.A. Segalman, S.C.B. Mannsfeld, and A. Salleo: Role of side-chain branching on thin-film structure and electronic properties of polythiophenes. *Adv. Funct. Mater.* (2015). doi:10.1002/adfm.201500101.
22. B.C. Schroeder, R.S. Ashraf, S. Thomas, A.J.P. White, L. Biniek, C.B. Nielsen, W. Zhang, Z. Huang, P.S. Tuladhar, S.E. Watkins, T.D. Anthopoulos, J.R. Durrant, and I. McCulloch: Synthesis of novel thieno[3,2-b]thienobis (silolothiophene) based low bandgap polymers for organic photovoltaics. *Chem. Commun.* **48**, 7699 (2012).
23. B.C. Schroeder, M. Kirkus, C.B. Nielsen, R.S. Ashraf, and I. McCulloch: Dithienosilolothiophene, a new polyfused donor for organic electronics, *submitted* (2015).
24. B.C. Schroeder, Z. Huang, R.S. Ashraf, J. Smith, P. D'Angelo, S.E. Watkins, T.D. Anthopoulos, J.R. Durrant, and I. McCulloch: Silaindacenodithiophene-based low band gap polymers—the effect of fluorine substitution on device performances and film morphologies. *Adv. Funct. Mater.* **22**, 1663 (2012).

https://doi.org/10.1557/mrc.2015.49 Published online by Cambridge University Press